HHS Public Access

Author manuscript

*Toxicol Lett*. Author manuscript; available in PMC 2020 October 01.

Published in final edited form as:

*Toxicol Lett*. 2020 October 01; 331: 82–91. doi:10.1016/j.toxlet.2020.05.023.

# Differential susceptibility of PC12 and BRL cells and the regulatory role of HIF-1α signaling pathway in response to acute methylmercury exposure under normoxia

**Tingting Liu**[a], **Qianqian Gao**[a], **Bobo Yang**[a], **Changsheng Yin**[b,a], **Jie Chang**[a], **Hai Qian**[a], **Guangwei Xing**[a], **Suhua Wang**[a], **Fang Li**[a], **Yubin Zhang**[c], **Da Chen**[d], **Jiyang Cai**[e], **Haifeng Shi**[b], **Michael Aschner**[f], **Kwaku Appiah-Kubi**[g], **Dawei He**[h], **Rongzhu Lu**[a,h,*]

[a]Department of Preventive Medicine and Public Health Laboratory Sciences, School of Medicine, Jiangsu University, Zhenjiang, Jiangsu 212013, China

[b]Institute of Life Sciences, Jiangsu University, Zhenjiang, Jiangsu 212013, China

[c]Department of Occupational Health and Toxicology, School of Public Health, Fudan University, Shanghai 200032, China

[d]School of Environment, Jinan University, Guangzhou, Guangdong 510632, China

[e]Department of Physiology, College of Medicine, University of Oklahoma Health Science Center, Lindsay, Oklahoma City, OK 73104, USA

[f]Department of Molecular Pharmacology, Albert Einstein College of Medicine, Bronx, NY 10461, USA

[g]Department of Applied Biology, University for Development Studies, Navrongo, Ghana

[h]Center for Experimental Research, Kunshan Hospital Affiliated to Jiangsu University, Kunshan, Jiangsu 215130, China

## Abstract

Hypoxia-inducible factor 1 (HIF-1) is a critical nuclear transcription factor for adaptation to hypoxia. HIF-1α, the regulatable subunit of HIF-1, is a cytoprotective factor that regulates various physiological activities. We used rat adrenal pheochromocytoma (PC12) cells and the rat hepatocyte cell line BRL to examine the effects of methylmercury (MeHg). Treatment with MeHg led to time- and concentration-dependent toxicity in both lines with statistically cytotoxic effects at 5 μM and 10 μM in PC12 and BRL, respectively, at 0.5 hours. The protein level of HIF-1α was significantly decreased at 2.5 and 5 μM MeHg in PC12 and BRL cells, respectively. Furthermore, MeHg reduced the protein levels of the HIF-1α target proteins glucose transporter-1, vascular endothelial growth factor–A and erythropoietin. Overexpression of HIF-1α significantly attenuated MeHg-induced toxicity in both cell types. Notably, cobalt chloride, a pharmacological inducer of HIF-1α, significantly attenuated MeHg-induced toxicity in BRL cells but not in PC12 cells. An inhibitor of prolyl hydroxylase (PHD), 3, 4-Dihydroxybenzoic acid (DHB), and the

*Corresponding author: Dr.Rongzhu Lu, Department of Preventive Medicine and Public Health Laboratory, Sciences, School of Medicine, Jiangsu University, 301 Xuefu Road, Zhenjiang, Jiangsu 212013, China, lurz@ujs.edu.cn, Tel: +86 511 85038449; Fax: +86 511 85038483.

proteasomes inhibitor MG132 antagonized the toxicity of MeHg in both cell lines. However, 2-Methoxyestradiol, a HIF-1α inhibitor, significantly increased MeHg-induced toxicity in both cell lines. These data establish that (a) neuronal PC12 cells are more sensitive to MeHg than non-neuronal BRL cells (b) HIF-1α plays a similar role in MeHg-induced toxicity in both cell lines and (c) upregulation of HIF-1α by different methods offers greater cytoprotection against the toxicity of MeHg in PC2 and BRL cell lines.

**Keywords**

Methylmercury; HIF-1α; PC12; BRL; Susceptibility

## 1. Introduction

Mercury is a naturally occurring element, found as both inorganic and organic form (Clarkson., 2002;Clarkson., 2006). The primary sources of mercury are man-made emissions from mining, coal burning and other fossil fuel byproducts (Streets et al., 2011). Microorganisms generate organic mercury including methylmercury (MeHg) by promoting the methylation of inorganic mercury, biologically enriching it through the food chain, especially in aquatic fish and mammals. MeHg is the most common form of organic mercury and represents the most considerable human health risk (Clarkson et al., 2006), notably via consumption of MeHg-adulterated fish and seafood (Mahaffey et al. 2004; Sunderland et al., 2018; Tang et al., 2018), especially during pregnancy (Rosa-Silva et al. 2019). Rice is another source of mercury exposure (Gong et al., 2018), especially in China (Zhang et al., 2010). The gastrointestinal tract absorbs approximately 95% of ingested MeHg and widely distributed to liver (López-Berenguer et al., 2019; Ji et al., 2006, Mori et al., 2007; Cuello et al., 2010; Macedo-Júnior et al., 2017), kidneys and the central nervous system (CNS) (Kershaw et al., 1980 ; Bridges et al., 2010; Khadra et al., 2019). MeHg toxicity in humans can lead reduction of peripheral vision, language impairment, hearing loss, memory loss and motor system disease (Goldberg, 2010; 1994; Grandjean et al., 2011). The mechanisms of the toxicity of MeHg have been linked to induction of oxidative stress (Chen et al., 2020), mitochondrial dysfunction (Qu et al., 2013) and calcium dyshomeostasis (Dreiem et al., 2007; Liu et al., 2019).

Toxic metals, such as cobalt (Lauryn et al., 2013; Bahadori et al., 2019), copper (Martin et al., 2005), nickel (Davidson et al., 2006), aluminum (Al) (Mailloux et al., 2009), and cadmium (Jing et al., 2012; Fujiki et al., 2017) stabilize HIF-1α. Stabilized HIF-1α dimerizes with HIF-1β, which can bind to hypoxia-response elements on target DNA to activate transcription of a series of downstream target genes, including glucose transporter-1 (GLUT-1) (Semenza and Wang., 1992; Hoskin et al., 2003), vascular endothelial growth factor-A (VEGF-A) (Pore et al., 2006; Xu et al.,2018) and erythropoietin (EPO) (Semenza et al., 1991). Upregulation of HIF-1α can significantly antagonize the toxicity of several drugs and toxins by regulating HIF-1α targets (Mailloux et al., 2011; Guo et al., 2016). Yasutake et al., (1997) found that prolonged exposure to MeHg was associated with anemic symptoms in humans, possibly related to the inhibition of EPO, a target of HIF-1α which is reported to play a neuroprotective role on neuronal damage via its anti-apoptotic action (Merelli et al.,

2019). Our previous study has proved that the toxicity of MeHg is closely related to the downregulation of HIF-1α (Chang et al., 2019). But the tissue-specific role of HIF-1α in antagonizing toxicity of MeHg remains unclear. The liver and brain are the primary sites of oxygen sensor expression and they also are the most active organs during metabolism and the brain is the first to be protected organs in response to hypoxia (Zhang et al., 2017). To have a complete picture, we thus examined the effect of MeHg on HIF-1α expression and further explored the role of HIF-1α in mediating cytotoxicity and cytoprotection in PC12 and BRL cells.

## 2. Materials and Methods

### 2.1 Chemicals and reagents

MeHg, cobalt chloride ($CoCl_2$), 3, 4-Dihydroxybenzoic acid (DHB), MG132, dimethyl sulfoxide (DMSO), and 3-(4, 5-dimethylthiazol-2-yl)-2, 5-diphenyl diphenyltetrazolium bromide (MTT) were purchased from Sigma–Aldrich (St. Louis, MO, USA), and 2-methoxyestradiol (2-MeOE2) was from Selleck Chemicals (Houston, TX, USA). For Western blot analysis, polyclonal antibodies to HIF-1α were obtained from ImmunoWay (Plano, TX, USA), while those for EPO, GLUT-1 and VEGF-A were obtained from ABclonal (Cambridge, MA, USA). Anti-HIF-1β and β-actin were purchased from Cell Signaling Technology (Danvers, MA, USA). Secondary antibodies were obtained from Santa Cruz Biotechnology (Santa Cruz, CA, USA). Nerve growth factor (NGF) was purchased from Harlan Laboratories (Houston, TX, USA).

### 2.2 Cell culture

PC12 is derived from a rat adrenal pheochromocytoma (Greene and Tischler, 1976). After exposure to nerve growth factor (NGF), PC12 cells undergo nerve differentiation (Greene et al., 1976; Parran et al., 2001), so we chose PC12 cells as neuronal cells. In our study, PC12 cells were differentiated in DMEM with 50 ng/ml nerve growth factor and 1 % fetal bovine serum for 9 days. To further assess the toxicity of MeHg to liver and compare the differences with the CNS, we chose normal rat liver cell line BRL cell as non-neuronal cells which is widely used in the study of hepatotoxicity (Liu et al., 2019). PC12 and BRL cells were purchased from the Institute of Cell Biology, Chinese Academy of Science (Shanghai, China). PC12 cells were induced to neuronal differentiation with nerve growth factor. Both cells were grown in high-glucose Dulbecco's modified Eagle's medium (DMEM) (Hyclone, Logan, UT, USA) supplemented with 10% fetal bovine serum (FBS) (Gibco, Thermo Fisher Scientific, Waltham, MA, USA). Cells were maintained at 37°C in a 5% $CO_2$ environment. The cultured cells were replaced with fresh media twice a week. Cultured cells were used for experiments when they reached 75–85% confluence.

### 2.3 MTT cell viability assay

Cells were seeded at $5 \times 10^3$ cells/well in 96-well plates, incubated for 24 h, then treated with MeHg (at the indicated concentrations) and other agents. PC12 and BRL cells were cultured in 96-well plates and treated with graded concentrations of MeHg (0, 1, 2.5, 5, 10 μM) for 0.5 to 6 h. After pretreatment with $CoCl_2$ (200 μM, 0.5 h), 2-MeOE2 (10 μM, 0.5 h), DHB (1 mM, 6 h) and MG132 (1 μM, 24 h), PC12 or BRL cells were washed twice with

phosphate-buffered saline (PBS) and incubated in fresh media with 10 μM MeHg for 0.5 h. MTT solution (0.5 mg/mL) was added to the MeHg-treated cells and incubated for an additional 4 h; the addition of DMSO dissolved dark-blue formazan crystals in viable cells, and the optical density at 490 nm was read with a Bio-Rad 680 Microplate Reader (Bio-Rad Laboratories, Hercules, CA, USA).

### 2.4 Lactate dehydrogenase (LDH) release assay

Cell cytotoxicity was determined using an LDH-release assay kit (Jiancheng Bioengineering Institute of Nanjing, Jiangsu, China). Cells ($1 \times 10^4$/well) were incubated in 24-well plates for 24 hours. Following MeHg treatment, intracellular LDH was released into the culture supernatant by damaged cells. The supernatant was transferred into 96-well plates and measured according to manufacturer's protocol. The absorbance was detected at 450 nm using a Bio-Rad 680 Microplate Reader. The absorbance value is proportional to the degree of cell damage. Control groups were treated with free media without any agents

### 2.5 Western blot analysis

To prepare whole protein lysates, the test cells grown in 6-well plates were washed three times with cold PBS, lysed in a radioimmunoprecipitation assay lysis buffer (RIPA) containing 1% phenylmethylsulfonyl fluoride (Beyotime, Shanghai, China), incubated on ice for 10–15 minutes, and collected by centrifugation at 12,000 g at 4°C for 15 minutes. The protein concentration was determined using a BCA protein assay reagent kit (Beyotime, Shanghai, China). Standard Western blotting procedure was as follows: extracted protein was subjected to SDS-PAGE and transferred to a polyvinylidene fluoride (PVDF) membrane (Millipore, Darmstadt, Germany). Membranes were blocked with 5% nonfat milk and incubated overnight at 4°C with primary antibodies including HIF-1α, GLUT-1, VEGF-A, EPO or β-actin. Membranes were then washed three times in TBST (10 mM Tris–HCl, 120 mM NaCl, 0.1% Tween-20, pH 7.4) buffer before incubation with the secondary antibody. The enhanced chemiluminescence method was used to develop the signals, and membranes were scanned with the MiniChemi Mini Size Chemiluminescent Imaging System (Beijing Sage Creation Science Co. Ltd, Beijing, China) and Image J software (National Institutes of Health, Bethesda, MD, USA) was used to analyze the band density.

### 2.6 Adenovirus transfection

Adenovirus carrying the HIF-1α gene was obtained from Hanbio Biotechnology Co., Ltd (Shanghai, China). The cells were seeded into 6-well plates with $5 \times 10^4$ cells/well and transfected with commercially available HIF-1α or control adenovirus according to MOI (multiplicity of infection=$100 \times 10^8$ PFU/mL following the manufacturer's instructions. Virus solution was diluted in serum-free DMEM medium, and then added to the 6-well plates and incubated at 37°C for 6 hours. The culture media containing the virus was removed and replaced with high-glucose DMEM containing 10% FBS. Experiments were carried out after 48 hours of culture.

### 2.7 Real-time reverse transcription-polymerase chain reaction (RT-PCR)

Total RNA was isolated from the cells using Trizol reagent. RNA samples (2 μg) were reverse-transcribed to generate first-strand cDNA. The primers for rat HIF-1α and β-actin were designed and synthesized by Shanghai Generay Biotech Co., Ltd (Shanghai, China). The following primers were used to amplify HIF-1α mRNA (forward, 5′-TCACAAATCAGCACCAAGCAC-3′; reverse: 5′-AAGGGGAAAGAACAAAACACG-3′) and β-actin mRNA as an internal standard (forward, 5′-CCTAGACTTCGAGCAAGAGA-3′; reverse, 5′-GGAAGGAAGGCTGGAAGA-3′). Fold changes in the expression of the HIF-1α gene were calculated using a comparative threshold cycle (Ct) method using the formula $2^{-(\Delta\Delta Ct)}$.

### 2.8 Statistical analysis

The results are presented as mean ± standard deviation. Statistical analyses employed a one-way analysis of variance followed by a Dunnett test, a multiple comparison procedure. The assays were repeated at least three times in at least three independently derived PC12 and BRL cell cultures. Significance was taken as $p < 0.05$.

## 3. Results

### 3.1 MeHg reduced cell viability and induced cytotoxicity in PC12 and BRL cells

MeHg caused a time- and concentration-dependent decrease in cell viability in both cell types. The half-maximal inhibitory concentration values of the MTT cell viability reduction varying intervals up to 6 hours in the presence of MeHg at 5 μM or 10 μM in PC12 and BRL cells, respectively. At the 0.5 h incubation, PC12 and BRL cell viability was decreased to 69.5 ± 2.4% and 77.9 ± 3.7% of controls, respectively ($p < 0.05$) (Fig. 1A). Accordingly, 0.5 h of treatment with 10 μM MeHg was used for subsequent experiments. LDH release was increased in a concentration-dependent manner and was significantly elevated relative to controls ($p < 0.05$) in PC12 cells treated for 0.5 hours with 2.5 μM MeHg and 10 μM MeHg in BRL cells (Fig. 1B). Accordingly, 0.5 h of treatment with 10 μM MeHg was used for subsequent experiments.

### 3.2 MeHg reduced the HIF-1α protein and its downstream targets, but did not affect the level of HIF-1α mRNA

To investigate whether the toxicity of MeHg was associated with altered the protein level of HIF-1α, PC12 and BRL cells were treated with MeHg (0, 1, 2.5, 5, 10 μM) for 0.5 h. The protein levels of HIF-1α and HIF-1β, the persistently expressed subunit that is also known as aryl hydrocarbon receptor nuclear translocator (ARNT), and the downstream targets of HIF-1α, GLUT-1, VEGF-A and EPO, were evaluated by Western blotting. As shown in Figure 2A, MeHg treatment for 0.5 h significantly reduced the protein level of HIF-1α at 2.5 μM in PC12 cells and 5 μM in BRL cells. With 2.5, 5, 10 μM MeHg, the protein level of HIF-1α decreased to ~12% and ~54% in PC12 and BRL cells, respectively. Measurement of HIF-1α mRNA using RT-PCR did not reveal significantly altered mRNA levels under treatment with MeHg (Fig. 2B). The levels of the HIF-1β did not change significantly after MeHg treatment (Fig. 2C), whereas the HIF-1α-targeted proteins VEGF-A, GLUT-1 and

EPO did decrease with increasing MeHg concentration (Fig. 2D). The decrease in HIF-1α was more pronounced in PC12 cells than that in BRL cells, consistent with the heightened sensitivity of PC12 to MeHg. Notably, MeHg decreased the protein levels of GLUT-1 at 1μM in PC12 and 5 μM in BRL cells.

### 3.3 Overexpression of recombinant HIF-1α attenuated MeHg-induced cytotoxicity in PC12 and BRL cells

To investigate the role of HIF-1α in MeHg-induced toxicity, we used genetic manipulation to overexpress HIF-1α. At an MOI of $100 \times 10^8$ PFU/mL, HIF-1α levels significantly increased compared with control (Fig. 3A). Compared with MeHg alone, pretreatment with adenoviral *HIF-1α* before treatment with MeHg significantly increased the protein level of HIF-1α and its downstream proteins (Fig. 3B–C). Overexpresssion of HIF-1α also attenuated the cytotoxicity induced by MeHg in both cell lines (Fig. 3D). These results indicated that the cytotoxicity of MeHg was significantly inhibited by the upregulation of HIF-1α in both cell types, establishing that MeHg-induced cytotoxicity can be antagonized by upregulating the protein level HIF-1α.

### 3.4 Pharmacological induction of HIF-1α and its targets by $CoCl_2$ protected BRL but not PC12 cells against MeHg-induced acute cytotoxicity

PC12 and BRL cells were treated with 10 μM MeHg for 0.5 hours after pretreatment with $CoCl_2$ (200 μM for 0.5 hours). $CoCl_2$ is commonly used to induce hypoxic conditions, which leads to the induction of HIF-1α protein (Tripathi et al., 2019; Yu et al., 2019). As shown in Figure 4A–B, the levels of HIF-1α, GLUT-1, VEGF-A and EPO significantly increased ($p < 0.05$) after pretreatment with $CoCl_2$ compared with MeHg alone. The viability of BRL cells upon pretreatment with $CoCl_2$ before MeHg was significantly increased ($p < 0.05$) compared with that under MeHg treatment alone (Fig. 4C). However, in PC12 cells, $CoCl_2$ pretreatment did not significantly enhance cell viability. These results indicated that $CoCl_2$ affords protection by inducing upregulation of HIF-1α in non-neuronal cells, but not neuronal cells which are more sensitive to oxygen-induced cytotoxicity.

### 3.5 Pharmacological induction of HIF-1α and its targets by DHB attenuated MeHg-induced acute cytotoxicity in PC12 and BRL cells

DHB was reported to act as an iron chelater and its inhibitory actions occur via the displacement of 2-oxoglutarate and ascorbate (Majamaa et al., 1986; Siddiq et al., 2005). Iron, 2-oxoglutarate and ascorbate are the important cofactor of PHD, so DHB is widely used as a PHD inhibitor in the study of upregulation of HIF-1α. Cells were pretreated with 1 mM 3, 4-Dihydroxybenzoic acid (DHB) for 6 hours, then treated with MeHg (10 μM, 0.5 hours). As shown in Figure 5A–B, compared with the control group, DHB alone significantly induced the protein levels of HIF-1α and its targets in both PC12 and BRL cells ($p < 0.05$), while the MeHg-treated group showed significant inhibition the protein levels of HIF-1α and its targets. Upon pretreatment with DHB, the levels of HIF-1α and its downstream targets GLUT-1, VEGF-A and EPO, were significantly higher than those in the MeHg-alone groups, both in PC12 and BRL cells. DHB also mitigated the MeHg-induced decrease in cell viability in PC12. An analogous response was also noted in BRL cells (Fig. 5C). DHB increased cell viability by ~ 15% and ~ 10% in MeHg-treated PC12 and BRL

cells, respectively. These results supported the notion that the protective effects of DHB against MeHg-induced cytotoxicity were due to the activation of HIF-1α pathway.

### 3.6 Pharmacological induction of HIF-1α and its targets by MG132 attenuated MeHg-induced acute cytotoxicity in PC12 and BRL cells

The 26s proteasome finally degrades PHD-hydroxylated HIF-1α after interaction with the von Hippel Lindau tumor suppressor protein (Schofield et al., 2004; Domene and Illingworth 2012). A blocker of the proteasome, MG132 (Wang et al., 2019), was used to investigate the protective role of HIF-1α in the toxicity of MeHg. MG132 was protects against the degradation of the HIF-1 complex in cells transferred from hypoxia to normoxia and is able to induce HIF-1 complex formation when added to normoxic cells (Salceda and Caro 1997). Cells were pretreated with MG132 at a concentration of 1 μM for 24 hours, and then treated with MeHg (10 μM, 0.5 hours). Western blotting analysis showed that, compared with the MeHg-treated group, MG132 significantly increased the protein levels of HIF-1α and its downstream targets GLUT-1, VEGF-A and EPO (Fig. 6A–B). Cell viability experiments showed that, compared with the control group, the viability in the MeHg group was significantly decreased. Compared with the MeHg treatment-alone group, HIF-1α overexpression by MG132 prevented MeHg-induced cell toxicity (Fig. 6C). MG132 increased cell viability by ~ 16% and ~ 8% in MeHg-treated PC12 and BRL cells, respectively.

### 3.7 2-MeOE2 decreased HIF-1α protein levels and its targets enhanced MeHg-induced cytotoxicity in both PC12 and BRL cells

To further investigate the role of HIF-1α in MeHg-induced toxicity, PC12 and BRL cells were pretreated with 2-MeOE2 (10 μM for 0.5 hours), an inhibitor of HIF-1α (Docherty et al., 2019), followed by treatment with MeHg (10 μM for 0.5 hours). The protein levels of HIF-1α and its downstream targets significantly decreased upon pretreatment with 2-MeOE2 ($p < 0.05$) compared with cells treated with MeHg alone (Fig. 7A–B). The viability of PC12 and BRL cells pretreated with 2-MeOE2 before MeHg was also significantly decreased ($p < 0.05$) compared with cells treated with MeHg alone (Fig. 7C). These results indicated that the inhibition of HIF-1α exaggerated MeHg-induced cytotoxicity in PC12 and BRL cells, further corroborating the cytoprotective role of HIF-1α.

## 4. Discussion

The present study shows that MeHg induced a time- and concentration-dependent decrease in cell viability in both PC12 and BRL cells. MeHg was toxic at lower concentrations in PC12 versus BRL cells. MeHg also decreased the protein levels of HIF-1α and its targets in a concentration-dependent manner. To further elucidate the relationship between MeHg toxicity and HIF-1α, we used both pharmacological ($CoCl_2$, DHB, MG132, 2MeOE2) and genetic interventions to upregulate or downregulate HIF-1α, and showed efficacy in antagonizing and exacerbating the toxicity of MeHg in both cell lines. Additionally, HIF-1α mRNA was detected with RT-PCR, establishing the inability of MeHg to affect transcription and suggesting that its effects are secondary to the promotion of HIF-1α degradation via enhanced activity of the PHD and the proteasomal function. These results demonstrate that

HIF-1α plays an essential protective role in MeHg-induced cytotoxicity, and that the protective role of HIF-1α is not cell-specific, although it is more pronounced in neuronal cells.

Over the past several decades, the mechanism(s) associated with MeHg toxicity have been continuously addressed but are yet to be fully understood. Overproduction of ROS and inactivation of the antioxidant defense system represents a key mechanism of MeHg-induced cytotoxicity (Ali et al., 1992; Chung et al., 2019; Xin et al., 2019). Recent reports have also established a role for HIF-1α in regulating ROS production (Li et al., 2019). Activation of HIF-1α may inhibit ROS production (Wang et al., 2018; Sun et al., 2019). And loss of HIF-1α has been reported to induce ROS production (Saito et al., 2015).

MeHg as a well-known pollutant poses a severe threat to human health (Driscoll et al., 2013; Chung et al., 2019). The central nervous system (CNS) is particularly vulnerable to MeHg (Grandjean et al., 2011; López-Berenguer et al., 2019) which may be related to accumulating large quantities of mercury compared with other organs (Gonzalez et al., 2005). Cell proliferation in the present study showed that PC12 was more sensitive to MeHg induced toxicity than BRL cells (Fig.1A–B). Miura., et al (1999) also use PC12 cells as neuronal cells and HeLa cells as non-neuronal cells, firstly proved that neuronal cells is more sensitively towards the toxicity of MeHg. As an essential detoxification organ (Spry et al., 1991; Goldstein et al., 1996), Maulvault et al., (2016) reported that liver has the highest rate of elimination of MeHg compared with brain may via promoting the demethylation of MeHg (Ung et al., 2010; Evans et al., 2016).

We also showed that MeHg led to the decreased of the protein levels of HIF-1α (Fig. 2A) and its targets (Fig. 2D–G) in both cells, and that the protein of HIF-1α was significantly decreased at a lower concentration of MeHg in PC12 cells, consistent with their heightened sensitivity to $O_2$ concentrations (Conrad et al., 2001). The lower protein levels of HIF-1α in PC12 cells after treatment with MeHg likely accounts for their heightened sensitivity to MeHg. The downregulation of HIF-1α upon exposure to MeHg may be multifactorial. MeHg-induced damage to the CNS and liver is associated with altered mitochondrial function (Lee et al., 2016; Tofighi et al., 2011; Mori et al., 2007) which leads to a pseudo-normoxic state with decreased consumption of $O_2$, and increased $O_2$ may cause the downregulation of HIF-1α (Ferlazzo et al., 2019). Second, damaged mitochondrial function leads to increased intracellular ROS levels, in turn altering HIF-1α protein levels (li et al., 2014; Movafagh et al., 2015; sun et al., 2019; Liu et al., 2020). Thirdly, impairment in mitochondrial function may lead to disordered glucose utilization, in turn downregulating HIF-1α levels by increasing 2-oxoglutarate, the cofactor of PHD (Dehne et al., 2010; Bergström et al., 2013).

Previous studies have established that PHD inhibitors afford neuroprotection against ischemic and anoxic stress in an HIF-1α dependent manner (Hyvarinen et al., 2010; Davis et al., 2018; Li et al., 2018). DHB, as an inhibitor of PHD, can reverse 1-methyl-4-phenyl-1, 2, 3, 6-tetrahydropyridine (MPTP)-induced dopaminergic neurodegeneration, secondary to the upregulation of HIF-dependent proteins, HO-1 and MnSOD (Lee et al., 2009). In our study, DHB attenuated the toxicity of MeHg in both cell lines, which might also be related to

HIF-1α and its downstream proteins (Fig. 4A–B). Cobalt chloride oxidizes iron and deactivates enzymes by destroying hydroxylase responsible for the degradation of HIF-1a, replacing iron at the active site of hydroxylase (Leggett 2008). Salnikow et al., (2004) suggest that oxidation/depletion of ascorbic acid also an important mechanism of cobalt chloride to affect the PHD enzymes. As a hypoxia mimic, $CoCl_2$ not only inducing the protein level of HIF-1α, but also inducing mitochondrial damage (López-Hernández et al., 2015), ATP depletion, and ROS production (Jones et al., 2013; Lauryn et al., 2013;). PC12 cells, representing a neuronal cell line, are more sensitive to decreased $O_2$ concentrations (Conrad et al., 2001) and require higher production of ATP. This concept as mentioned above might be the underlying mechanism why $CoCl_2$ showed high efficacy in attenuating MeHg-induced toxicity in BRL cells but failed to do so in PC12 cells (Fig. 3C). HIF-1α is hydroxylated by PHD, resulting in its ubiquitination by the von Hippel Lindau E3 ubiquitin ligase and subsequent degradation by the proteasome (Harten et al., 2010). MG132 as an inhibitor of the proteasome could inhibit chymotrypsin-like (ChTL) activity which is a novel approach to the treatment of stroke therapy and other diseases of the central nervous system (Wojcik et al., 2004; Chen et al., 2015). In our study, MG132 also significantly prevented the toxicity of MeHg by blocked MeHg-induced HIF-1α depletion, which further proves the cytoprotective effect of MG132. Upregulation of HIF-1α significantly antagonized the toxic effects of MeHg but not completely abated the toxic effects, suggesting that other mechanisms are involved in the toxicity of MeHg which should be further explored.

## 5. Conclusion

MeHg had a differential toxic effect on neuron-like and non-neuronal cells that may be related to the extent of downregulation of HIF-1α. HIF-1α overexpression may play a similar protective role against MeHg induced toxicity to different organs. But more specific indicators such as dopamine in the nervous system and transaminase in the liver system are needed to explore the different sensibility towards the toxicity of MeHg in different cell lines. And additional cell lines and animal models are needed to determine if HIF-1α is a novel and general target for therapeutic intervention in response to MeHg-induced toxicity.

## Acknowledgments

We thank Dr. Peter Spencer at Oregon Health & Science University for critical comments. This work was supported in part by the Natural Science Foundation of China (No. 30872139, 81273124, 31100964) and R01 ES07331, R01 ES10563, and ES020852 from the National Institute of Environmental Health Sciences (NIEHS).

## Abbreviations

| | |
|---|---|
| **2-MeOE2** | 2-Methoxyestradiol |
| **$CoCl_2$** | Cobalt chloride |
| **DHB** | 3, 4-Dihydroxybenzoic acid |
| **DMSO** | Dimethyl sulfoxide |
| **EPO** | Erythropoietin |

| | |
|---|---|
| **GLUT-1** | Glucose transporter 1 |
| **h** | Hour(s) |
| **HIF-1α** | Hypoxia-inducible factor-1α |
| **HIF-1β** | Hypoxia-inducible factor-1β |
| **LDH** | Lactate dehydrogenase |
| **MeHg** | Methylmercury |
| **MG132** | Carbobenzoxy-L-leucyl-L-leucyl-L-leucinal (Proteasome inhibitor) |
| **MTT** | 3-(4,5-dimethylthiazol-2-yl)-2,5-diphenyl diphenyltetrazolium bromide |
| **PHD** | prolyl hydroxylase |
| **ROS** | Reactive oxygen species |
| **VEGF-A** | Vascular endothelial growth factor A |
| **CNS** | Central nervous system |

## References


Ali SF., LeBel CP, Bondy SC, 1992 Reactive oxygen species formation as a biomarker of methylmercury and trimethyltin neurotoxicity. Neurotoxicology 13(3), 637–648. 10.1016/0168-0102(92)90073-L [PubMed: 1475065]

Bahadori MB, Vandghanooni S, Dinparast L, Eskandani M, Ayatollahi SA, Ata A, Nazemiyeh H, 2019 Triterpenoid corosolic acid attenuates HIF-1 stabilization upon cobalt (II) chloride-induced hypoxia in A549 human lung epithelial cancer cells. Fitoterapia. 134, 493–500. 10.1016/j.fitote.2019.03.013 [PubMed: 30898728]

Bergström AL, Fog K, Sager TN, Bruun AT, Thirstrup K, 2013 Competitive HIF Prolyl Hydroxylase Inhibitors Show Protection against Oxidative Stress by a Mechanism Partially Dependent on Glycolysis. ISRN Neurosci. 2013, 1–11. 10.1155/2013/598587

Bridges CC, Zalups RK, 2010 Transport of inorganic mercury and methylmercury in target tissues and organs. J Toxicol Environ Health B Crit Rev 13(5). 385–410 10.1080/10937401003673750 [PubMed: 20582853]

Chang J, Yang B, Zhou Y, Yin C, Liu T, Qian H, Xing G, Wang S, Li F, Zhang Y, Chen D, Aschner M, Lu R, 2019 Acute Methylmercury Exposure and the Hypoxia-Inducible Factor-1α Signaling Pathway under Normoxic Conditions in the Rat Brain and Astrocytes in Vitro. Environ Health Perspect 7, 127006 10.1289/EHP5139. Epub 2019 Dec 18

Chen N, Tang X, Ye Z, Wang S, Xiao X, 2020 Methylmercury disrupts autophagic flux by inhibiting autophagosome-lysosome fusion in mouse germ cells. Ecotoxicol. Environ. Saf 198, 110667 10.1016/j.ecoenv.2020.110667 [PubMed: 32339925]

Chen X, Zhang X, Wang Y, Lei H, Huang R, 2015 Inhibition of immunoproteasome reduces infarction volume and attenuates inflammatory reaction in a rat model of ischemic stroke. Cell Death Dis 6, e1626 10.1038/cddis.2014.586 [PubMed: 25633295]

Chung YP, Yen CC, Tang FC, Lee KI, Liu SH, Wu CC, Hsieh SS, Su CC, Kuo CY, Chen YW, 2019 Methylmercury exposure induces ROS/Akt inactivation-triggered endoplasmic reticulum stress-regulated neuronal cell apoptosis. Toxicology 425, 152245 10.1016/j.tox.2019.152245 [PubMed: 31330229]

Clarkson TW, 2002 The three modern faces of mercury. Environ. Health Perspect 110, 11–23. 10.1016/10.1289/ehp.02110s111 [PubMed: 11834460]

Clarkson TW, Magos L, 2006 The toxicology of mercury and its chemical compounds. Crit Rev Toxicol. 36(8), 609–662. 10.1016/j.envres.2017.08.051 [PubMed: 16973445]

Conrad PW, Conforti L, Kobayashi S, Beitner-Johnson D, Rust RT, Yuan Y, Kim HW, Kim RH, Seta K, Millhorn DE, 2001 The molecular basis of O2-sensing and hypoxia tolerance in pheochromocytoma cells. Comp. Biochem. Physiol. B, Biochem. Mol. Biol 128(2):187–204. 10.1016/s1096-4959(00)00326-2 [PubMed: 11207433]

Cuello S, Goya L, Madrid Y, Campuzano S, Pedrero M, Bravo L, Cámara C, Ramos S, 2010 Molecular mechanisms of methylmercury-induced cell death in human HepG2 cells. Food Chem. Toxicol 48(5), 1405–1411. 10.1016/j.fct.2010.03.009 [PubMed: 20226830]

Davidson TL, Chen H, Di Toro DM, D'Angelo G, Costa M, 2006 Soluble nickel inhibits HIF-prolyl-hydroxylases creating persistent hypoxic signaling in A549 cells. Mol Carcinog 45(7), 479–489. 10.1002/mc.20176. [PubMed: 16649251]

Davis CK, Jain SA, Bae ON, Majid A, Rajanikant GK, 2018 Hypoxia Mimetic Agents for Ischemic Stroke. Front Cell Dev Biol. 6, 175 10.3389/fcell.2018.00175 [PubMed: 30671433]

Dehne N, Hintereder G, Brüne B, 2010 High glucose concentrations attenuate hypoxia-inducible factor-1α protein levels and signaling in non-tumor cells. Exp. Cell Res 316(7), 1179–1189. 10.1016/j.yexcr.2010.02.019 [PubMed: 20184881]

Docherty CK, Nilsen M, MacLean MR, 2019 Influence of 2-Methoxyestradiol and Sex on Hypoxia-Induced Pulmonary Hypertension and Hypoxia-Inducible Factor-1-α. J Am Heart Assoc. 8(5), e011628 10.1161/JAHA.118.011628 [PubMed: 30819028]

Domene C, Illingworth CJ, 2012 Effects of point mutations in pVHL on the binding of HIF-1α. Proteins. 80(3), 733–746. 10.1002/prot.23230 [PubMed: 22105711]

Dreiem A, Seegal RF, 2007 Methylmercury-induced changes in mitochondrial function in striatal synaptosomes are calcium-dependent and ROS-independent. Neurotoxicology. 28(4), 720–726. 10.1016/j.neuro.2007.03.004 [PubMed: 17442395]

Driscoll CT, Mason RP, Chan HM, Jacob DJ, Pirrone N, 2013 Mercury as a Global Pollutant: Sources, Pathways, and Effects. Environ. Sci. Technol 47(10), 4967–4983. 10.1021/es305071v [PubMed: 23590191]

Evans RD, Hickie B, Rouvinen-Watt K, Wang W, 2016 Partitioning and kinetics of methylmercury among organs in captive mink (Neovison vison): A stable isotope tracer study. Environ. Toxicol. Pharmacol 42, 163–169. 10.1016/j.etap.2016.01.007 [PubMed: 26855415]

Ferlazzo N, Curro M,Giunta ML, Longo D, Rizzo V, Caccamo D, Ientile R, 2020 Up-regulation of HIF-1α is associated with neuroprotective effects of agmatine against rotenone-induced toxicity in differentiated SH-SY5Y cells. Amino Acids. 52(2):171–179. 10.1007/s00726-019-02759-6 [PubMed: 31292720]

Fujiki K, Inamura H, Miyayama T, Matsuoka M, 2017 Involvement of Notch1 signaling in malignant progression of A549 cells subjected to prolonged cadmium exposure. J. Biol. Chem 292(19), 7942–7953. 10.1074/jbc.M116.759134 [PubMed: 28302721]

Goldberg D, 2010 Critical reviews in clinical laboratory sciences. Crit Rev Clin Lab Sci. 47(1), 1–4. 10.3109/10408360903507283. [PubMed: 20205625]

Goldstein RM, Brigham ME, Stauffer JC, 1996 Comparison of Mercury Concentrations in Liver, Muscle, Whole Bodies, and Composites of Fish from the Red River of the North. Can. J. Fish. Aquat. Sci 53(2), 244–252. 10.1139/cjfas-53-2-244

Gong Y, Nunes LM, Greenfield BK, Qin Z, Yang Q, Huang L, Bu W, Zhong H, 2018 Bioaccessibility-corrected risk assessment of urban dietary methylmercury exposure via fish and rice consumption in China. Sci. Total Environ 630, 222–230. 10.1016/j.scitotenv.2018.02.224 [PubMed: 29477821]

Gonzalez P, Dominique Y, Massabuau JC, Boudou A, Bourdineaud JP, 2005 Comparative effects of dietary methylmercury on gene protein levels in liver, skeletal muscle, and brain of the zebrafish (Danio rerio). Environ. Sci. Technol 39(11), 3972–3980. 10.1021/es0483490 [PubMed: 15984772]

Grandjean P, Herz KT, 2011 Methylmercury and brain development: imprecision and underestimation of developmental neurotoxicity in humans. Mt. Sinai J. Med 78(1), 107–118. [PubMed: 21259267]

Greene LA, Tischler AS, 1976 Establishment of a noradrenergic clonal line of rat adrenal pheochromocytoma cells which respond to nerve growth factor. Proc. Natl. Acad. Sci. U.S.A 73(7), 2424–2428. 10.1073/pnas.73.7.2424 [PubMed: 1065897]

Guo C, Hao LJ, Yang ZH, Chai R, Zhang S, Gu Y, Gao HL, Zhong ML, Wang T, Li JY, Wang ZY, 2016 Deferoxamine-mediated up-regulation of HIF-1α prevents dopaminergic neuronal death via the activation of MAPK family proteins in MPTP-treated mice. Exp. Neurol 280, 13–23. 10.1016/j.expneurol [PubMed: 26996132]

Harten SK, Ashcroft M, Maxwell PH, 2010 Prolyl hydroxylase domain inhibitors: a route to HIF activation and neuroprotection. Antioxid. Redox Signal 12(4), 459–480. 10.1089/ars.2009.2870 [PubMed: 19737089]

Hoskin PJ, Sibtain A, Wilson GD, 2003 GLUT1 and CAIX as intrinsic markers of hypoxia in bladder cancer: relationship with vascularity and proliferation as predictors of outcome of ARCON. Br. J. Cancer 89(7), 1290–1297. 10.1038/sj.bjc.6601260 [PubMed: 14520462]

Hyvarinen J, Hassinen IE, Sormunen R, Mäki JM, Kivirikko KI, Koivunen P, Myllyharju J, 2010 Hearts of hypoxia-inducible factor prolyl 4-hydroxylase-2 hypomorphic mice show protection against acute ischemia-reperfusion injury. J. Biol. Chem 285(18), 13646–13657. 10.1074/jbc.M109.084855 [PubMed: 20185832]

Ji X, Wang W, Cheng J, Yuan T, Zhao X, Zhuang H, Qu L, 2006 Free radicals and antioxidant status in rat liver after dietary exposure of environmental mercury. Environ. Toxicol. Pharmacol 22(3), 309–314. 10.1016/j.etap.2006.05.004 [PubMed: 21783725]

Jing Y, Liu LZ, Jiang Y, Zhu Y, Guo NL, Barnett J, Rojanasakul Y, Agani F, Jiang BH, 2012 Cadmium increases HIF-1 and VEGF protein levels through ROS, ERK, and AKT signaling pathways and induces malignant transformation of human bronchial epithelial cells. Toxicol. Sci 125(1), 10–19. 10.1093/toxsci/kfr256 [PubMed: 21984483]

Jones SM, Novak AE, Elliott JP, 2013 The role of HIF in cobalt-induced ischemic tolerance. Neuroscience. 252, 420–430. 10.1016/j.neuroscience.2013.07.060 [PubMed: 23916558]

Kershaw TG, Dhahir PH, Clarkson TW, 1980 The Relationship between Blood Levels and Dose of Methylmercury in Man. Arch. Environ. Health 35(1), 28–36. 10.1080/00039896.1980.10667458 [PubMed: 7189107]

Khadra M, Planas D, Brodeur P, Amyot M, 2019 Mercury and selenium distribution in key tissues and early life stages of Yellow Perch (Perca flavescens). Environ. Pollut 254, 112963 10.1016/j.envpol.2019.112963 [PubMed: 31377336]

Lauryn S, Caicedo MS, Seung-Jae L, Craig DV, Joshua J, Hallab NJ, 2013 Cobalt-Alloy Implant Debris Induce HIF-1α Hypoxia Associated Responses: A Mechanism for Metal-Specific Orthopedic Implant Failure. Plos One, 8(6), e67127 10.1371/journal.pone.0067127 [PubMed: 23840602]

Lee DW, Rajagopalan S, Siddiq A, Gwiazda R, Yang L, Beal MF, Ratan RR, Andersen JK, 2009 Inhibition of Prolyl Hydroxylase Protects against 1-Methyl-4-phenyl-1,2,3,6-tetrahydropyridine-induced Neurotoxicity. J. Biol. Chem 284(42), 29065–29076. 10.1074/jbc.M109.000638 [PubMed: 19679656]

Lee JY, Ishida Y, Takahashi T, Naganuma A, Hwang GW, 2016 Transport of pyruvate into mitochondria is involved in methylmercury toxicity. Sci Rep 6, 21528 10.1038/srep21528 [PubMed: 26899208]

Leggett RW, 2008 The biokinetics of inorganic cobalt in the human body. The Sci. Total Environ 389, 259–269. 10.1016/j.scitotenv.2007.08.054 [PubMed: 17920105]

Li HS, Zhou YN, Li L, Li SF, Long D, Chen XL, Zhang JB, Feng L, Li YP, 2019 HIF-1α protects against oxidative stress by directly targeting mitochondria. Redox Biol. 25, 101109 10.1016/j.redox.2019.101109 [PubMed: 30686776]

Li X, Cui XX, Chen YJ, Wu TT, Xu H, Yin H, Wu YC, 2018 Therapeutic Potential of a Prolyl Hydroxylase Inhibitor FG-4592 for Parkinson's Diseases in Vitro and in Vivo: Regulation of Redox Biology and Mitochondrial Function. Front Aging Neurosci. 10, 121 10.3389/fnagi.2018.00121 [PubMed: 29755339]

Li YN, Xi MM, Guo Y, Hai CX, Yang WL, Qin XJ, 2014 NADPH oxidase-mitochondria axis-derived ROS mediate arsenite-induced HIF-1α stabilization by inhibiting prolyl hydroxylases activity. Toxicol. Lett 224(2), 165–174. 10.1016/j.toxlet.2013.10.029 [PubMed: 24188932]

Liu Z, Huang Y, Jiao Y, Chen Q, Wu D, Yu P, Li Y, Cai M, Zhao Y, 2020 Polystyrene nanoplastic induces ROS production and affects the MAPK-HIF-1/NFkB-mediated antioxidant system in Daphnia pulex. aquatic toxicology 220 10.1016/j.aquatox.2020.105420

Liu A, Sun Y, Wang X, Ihsan A, Tao Y, Chen D, Peng D, Wu Q, Wang X, Yuan Z, 2019 DNA methylation is involved in pro-inflammatory cytokines protein levels in T-2 toxin-induced liver injury. Food Chem. Toxicol 132, 110661 10.1016/j.fct.2019.110661 [PubMed: 31279042]

López-Berenguer G, Peñalver J, Martínez-López E, 2019 A critical review about neurotoxic effects in marine mammals of mercury and other trace elements. Chemosphere. 246, 125688 10.1016/j.chemosphere.2019.125688 [PubMed: 31896013]

López-Hernández B, Ceña V, Posadas I, 2015 The endoplasmic reticulum stress and the HIF-1 signalling pathways are involved in the neuronal damage caused by chemical hypoxia. Br. J. Pharmacol 172(11), 2838–2851. 10.1111/bph.13095 [PubMed: 25625917]

Macedo-Júnior SJ, Luiz-Cerutti M, Nascimento DB, Farina M, Soares Santos AR, de Azevedo Maia AH, 2017 Methylmercury exposure for 14 days (short-term) produces behavioral and biochemical changes in mouse cerebellum, liver, and serum. J. Toxicol. Environ. Health Part A 80, 1145–1155. 10.1080/15287394.2017.1357324 [PubMed: 28850017]

Mahaffey KR, Clickner RP, Bodurow CC, 2004 Blood organic mercury and dietary mercury intake: National Health and Nutrition Examination Survey, 1999 and 2000. Environ. Health Perspect 112(5), 562–770. 10.1289/ehp.6587 [PubMed: 15064162]

Mailloux RJ, Lemire J, Appanna VD, 2011 Hepatic response to aluminum toxicity: dyslipidemia and liver diseases. Exp. Cell Res 317(16), 2231–2238. 10.1016/j.yexcr.2011.07.009 [PubMed: 21787768]

Mailloux RJ, Puiseux-Dao S, Appanna VD, 2009 α-Ketoglutarate abrogates the nuclear localization of HIF-1α in aluminum-exposed hepatocytes. Biochimie. 91(3), 408–415. 10.1016/j.biochi.2008.10.014 [PubMed: 19028544]

Majamaa K, Gunzler V, Hanauske-Abel HM, Myllyla R, Kivirikko KI, 1986 Partial identity of the 2-oxoglutarate and ascorbate binding sites of prolyl 4-hydroxylase. J. Biol. Chem 261, 7819–7823. [PubMed: 3011801]

Martin F, Linden T, Katschinski DM, Oehme F, Flamme I, Mukhopadhyay CK, Eckhardt K, Tröger J, Barth S, Camenisch G, Wenger RH, 2005 Copper-dependent activation of hypoxia-inducible factor (HIF)-1: implications for ceruloplasmin regulation. Blood. 105(12), 4613–4619. 10.1182/blood-2004-10-3980 [PubMed: 15741220]

Maulvault AL, Custodio A, Anacleto P, Repolho T, Pousao P, Nunes ML, Diniz M, Rosa R, Marques A, 2016 Bioaccumulation and elimination of mercury in juvenile seabass (Dicentrarchus labrax) in a warmer environment. Environ Res. 149, 77–85. 10.1016/j.envres.2016.04.035 [PubMed: 27179934]

Merelli A, Ramos AJ, Lazarowski A, Auzmendi J, 2019 Convulsive Stress Mimics Brain Hypoxia and Promotes the P-Glycoprotein (P-gp) and Erythropoietin Receptor Overprotein levels. Recombinant Human Erythropoietin Effect on P-gp Activity. Front Neurosci 13, 750 10.3389/fnins.2019.00750 [PubMed: 31379495]

Miura K, Koide N, Himeno S, Nakagawa I, Imura N, 1999 The involvement of microtubular disruption in methylmercury-induced apoptosis in neuronal and nonneuronal cell lines. Toxicol. Appl. Pharmacol 160(3), 279–288. 10.1006/taap.1999.8781 [PubMed: 10544062]

Mori N, Yasutake A, Hirayama K, 2007 Comparative study of activities in reactive oxygen species production/defense system in mitochondria of rat brain and liver, and their susceptibility to methylmercury toxicity. Arch. Toxicol 81(11), 769–776. https://doi.org/0.1007/s00204-007-0209-2 [PubMed: 17464500]

Movafagh S, Crook S, Vo K 2015 Regulation of hypoxia-inducible factor-1a by reactive oxygen species: new developments in an old debate. Journal of cellular biochemistry 116, 696–703. 10.1002/jcb.25074 [PubMed: 25546605]

Parran DK, Mundy WR, Barone S, 2001 Effects of Methylmercury and Mercuric Chloride on Differentiation and Cell Viability in PC12 Cells. Toxicol Sci. 59(2), 278–290. 10.1093/toxsci/59.2.278 [PubMed: 11158721]

Pore N, Jiang Z, Gupta A, Cerniglia G, Kao GD, Maity A, 2006 EGFR tyrosine kinase inhibitors decrease VEGF protein levels by both hypoxia-inducible factor (HIF)-1-independent and HIF-1-dependent mechanisms. Cancer Res. 66(6), 3197–3204. 10.1158/0008-5472 [PubMed: 16540671]

Qu M, Nan X, Gao Z, Guo B, Liu B, Chen Z, 2013 Protective effects of lycopene against methylmercury-induced neurotoxicity in cultured rat cerebellar granule neurons. Brain Res. 1540, 92–102. 10.1016/j.brainres.2013.10.005 [PubMed: 24120987]

Rosa-Silva HTD, Panzenhagen AC, Schmidtt V, Alves Teixeira A, Espitia-Pérez P, de Oliveira Franco Á, Mingori M, Torres-Ávila JF, Schnorr CE, Hermann PRS, Moraes DP, Almeida RF, Moreira JCF, 2019 Hepatic and neurobiological effects of foetal and breastfeeding and adulthood exposure to methylmercury in Wistar rats. Chemosphere. 244, 125400 10.1016/j.chemosphere.2019.125400 [PubMed: 31809933]

Saito S, Lin YC, Tsai MH, Lin CS, Murayama Y, Sato R, Yokoyama KK, 2015 Emerging roles of hypoxia-inducible factors and reactive oxygen species in cancer and pluripotent stem cells. Kaohsiung J. Med. Sci 31(6), 279–286. 10.1016/j.kjms.2015.03.002 [PubMed: 26043406]

Salceda S, Caro J, 1997 Hypoxia-inducible factor 1alpha (HIF-1alpha) protein is rapidly degraded by the ubiquitin-proteasome system under normoxic conditions. Its stabilization by hypoxia depends on redox-induced changes. J. Biol. Chem 272(36), 22642–22647. 10.1074/jbc.272.36.22642 [PubMed: 9278421]

Salnikow K, Donald SP, Bruick RK, Zhitkovich A, Phang JM, Kasprzak KS, 2004 Depletion of Intracellular Ascorbate by the Carcinogenic Metals Nickel and Cobalt Results in the Induction of Hypoxic Stress. J. Biol. Chem 279(39), 40337–40344. 10.1074/jbc.M403057200 [PubMed: 15271983]

Schofield CJ, Ratcliffe PJ, 2004 Oxygen sensing by HIF hydroxylases. Nature Nat. Rev. Mol. Cell Biol 5(5), 343–354. 10.1038/nrm1366

Semenza GL, Nejfelt MK, Chi SM, Antonarakis SE, 1991 Hypoxia-inducible nuclear factors bind to an enhancer element located 3” to the human erythropoietin gene. Proc. Natl. Acad. Sci. U.S.A 88(13), 5680–5684. 10.1073/pnas.88.13.5680 [PubMed: 2062846]

Semenza GL, Wang GL, 1992 A nuclear factor induced by hypoxia via de novo protein synthesis binds to the human erythropoietin gene enhancer at a site required for transcriptional activation. Mol. Cell. Biol 12(12), 5447–5454. 10.1128/mcb.12.12.5447 [PubMed: 1448077]

Siddiq A, Ayoub IA, Chavez JC, Aminova L, Shah S, LaManna JC, Patton SM, Connor JR, Cherny RA, Volitakis I, Bush AI, Langsetmo I, Seeley T, Gunzler V, Ratan RR, 2005 Hypoxia-inducible factor prolyl 4-hydroxylase inhibition. A target for neuroprotection in the central nervous system. J. Biol. Chem 280(50), 41732–41743, 10.1074/jbc.M504963200 [PubMed: 16227210]

Spry DJ, Wiener JG, 1991 Metal bioavailability and toxicity to fish in low-alkalinity lakes: A critical review. Environ. Pollut 71, 243–304. 10.1016/0269-7491(91)90034-T [PubMed: 15092121]

Streets DG, Devane MK, Lu Z, Bond TC, Sunderland EM, Jacob DJ, 2011 All-time releases of mercury to the atmosphere from human activities. Environ. Sci. Technol 45(24), 10485–10491. 10.1021/es202765m [PubMed: 22070723]

Sun R, Meng X, Pu Y, Sun F, Man Z, Zhang J, Yin L, Pu Y, 2019 Overprotein levels of HIF-1a could partially protect K562 cells from 1, 4-benzoquinone induced toxicity by inhibiting ROS, apoptosis and enhancing glycolysis. Toxicol In Vitro. 55, 18–23. 10.1016/j.tiv.2018.11.005 [PubMed: 30448556]

Sun W, Wang B, Qu XL, Zheng BQ, Huang WD, Sun ZW, Wang CM, Chen Y, 2019 Metabolism of Reactive Oxygen Species in Osteosarcoma and Potential Treatment Applications. Cells. 9(1), 87 10.3390/cells9010087

Sunderland EM, Li M, Bullard K, 2018 Decadal Changes in the Edible Supply of Seafood and Methylmercury Exposure in the United States. Environ. Health Perspect 126(1), 017006 10.1289/EHP2644 [PubMed: 29342451]

Tang Z, Fan F, Wang X, Shi X, Deng S, Wang D, 2018 Mercury in rice and rice-paddy soils under long-term fertilizer and organic amendment. Ecotoxicol. Environ. Saf 150, 116–122. 10.1016/j.ecoenv.2017.12.021 [PubMed: 29272715]

Tofighi R, Johansson C, Goldoni M, Ibrahim WN, Gogvadze V, Mutti A, Ceccatelli S, 2011 Hippocampal neurons exposed to the environmental contaminants methylmercury and polychlorinated biphenyls undergo cell death via parallel activation of calpains and lysosomal proteases. Neurotox Res. 19(1), 183–194. 10.1007/s12640-010-9159-1 [PubMed: 20169435]

Tripathi VK, Subramaniyan SA, Hwang I, 2019 Molecular and Cellular Response of Co-cultured Cells toward Cobalt Chloride (CoCl)-Induced Hypoxia. ACS Omega. 4(25), 20882–20893. 10.1021/acsomega.9b01474 [PubMed: 31867478]

Ung CY, Lam SH, Hlaing MM, Winata CL, Korzh S, Mathavan S, Gong Z, 2010 Mercury-induced hepatotoxicity in zebrafish: in vivo mechanistic insights from transcriptome analysis, phenotype anchoring and targeted gene protein levels validation. BMC Genomics. 11, 212 10.1186/1471-2164-11-212 [PubMed: 20353558]

Wang G,, Li Y,, Yang Z,, Xu W,, Yang Y,, Tan X., 2018 ROS mediated EGFR/MEK/ERK/HIF-1α Loop Regulates Glucose metabolism in pancreatic cancer. Biochem. Biophys. Res. Commun 500(4), 873–878. 10.1016/j.bbrc.2018.04.177 [PubMed: 29702094]

Wang L, Liang Y, Li P, Liang Q, Sun H, Xu D, Hu W, 2019 Oncogenic Activities Of UBE2S Mediated By VHL/HIF-1α/STAT3 Signal Via The Ubiquitin-Proteasome System In PDAC. Onco Targets Ther. 12, 9767–9781. 10.2147/OTT.S228522 [PubMed: 31814735]

Wojcik C, Di Napoli M, 2004 Ubiquitin-proteasome system and proteasome inhibition: new strategies in stroke therapy. Stroke. 35(6), 1506–1518. 10.1161/01.STR.0000126891.93919.4e [PubMed: 15118168]

Xin R, Pan YL, Wang Y, Wang SY, Wang R, Xia B, Qin RN, Fu Y, Wu YH, 2019 Nickel-refining fumes induce NLRP3 activation dependent on mitochondrial damage and ROS production in Beas-2B cells. Arch. Biochem. Biophys 676, 108148 https://doi.org/10:108148 [PubMed: 31606392]

Xu Y, Lu X, Hu Y, Yang B, 2018 Melatonin attenuated retinal neovascularization and neuroglial dysfunction by inhibition of HIF-1α-VEGF pathway in oxygen-induced retinopathy mice. Journal of pineal research 64, e12473 10.1111/jpi.12473 [PubMed: 29411894]

Yasutake A, Nakano A, Miyamoto K, Eto K, 1997 Chronic effects of methylmercury in rats. I. Biochemical aspects. Tohoku J. Exp. Med 182(3), 185–196. 10.1620/tjem.182.185 [PubMed: 9362101]

Yu X, Wan Q, Ye X, Cheng Y, Pathak JL, Li Z, 2019 Cellular hypoxia promotes osteogenic differentiation of mesenchymal stem cells and bone defect healing via STAT3 signaling. Cell. Mol. Biol. Lett 24, 64 10.1186/s11658-019-0191-8 [PubMed: 31827540]

Zhang G, Zhao C, Wang Q, Gu Y, Li Z, Tao P, Chen J, Yin S, 2017 Identification of HIF-1 signaling pathway in Pelteobagrus vachelli using RNA-Seq: effects of acute hypoxia and reoxygenation on oxygen sensors, respiratory metabolism, and hematology indices. J. Comp. Physiol. B, Biochem. Syst. Environ. Physiol 187(7), 931–943. 10.1007/s00360-017-1083-8

Zhang H, Feng X, Larssen T, Qiu G, Vogt RD, 2010 In inland China, rice, rather than fish, is the major pathway for methylmercury exposure. Environ. Health Perspect 118(9), 1183–1188. 10.1289/ehp.1001915 [PubMed: 20378486]

## Highlights

- Neuronal PC12 cells were more sensitive than BRL cells to the toxicity of MeHg
- MeHg decreased HIF-1α in PC12 cells with a lower concentration than that in BRL cells
- Up-regulation of HIF-1α could antagonize the toxicity of MeHg in both cell lines

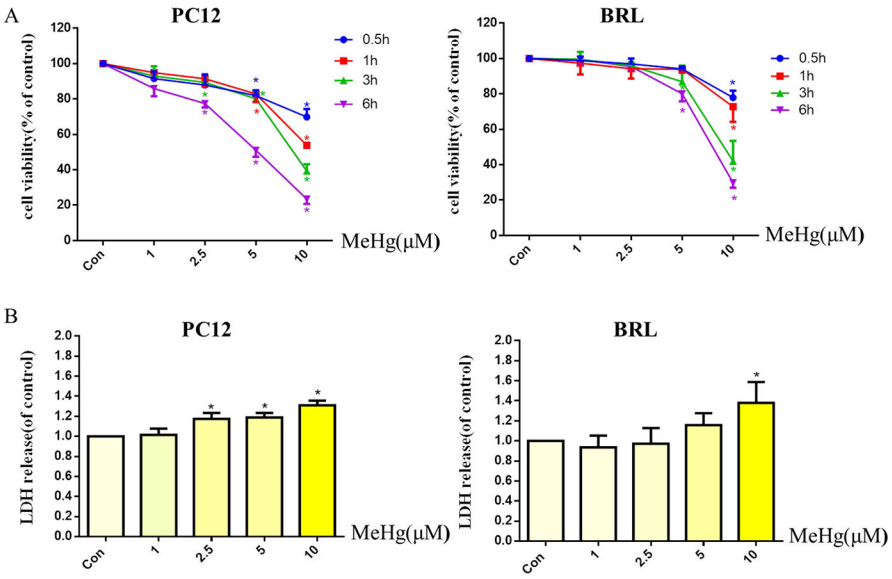


**Fig. 1.**

Effects of methylmercury (MeHg) on cell viability and cytotoxicity in PC12 and BRL cells. PC12 and BRL cells were treated with various concentrations (1–10 μM) of MeHg for 0.5 to 6 h. Cell viability (A) was measured by the MTT assay and cytotoxicity (B) was detected via lactate dehydrogenase (LDH) release. Data show mean ± standard deviation ($n = 3$). *$p < 0.05$, compared with the control group. Statistical analysis was performed by one-way analysis of variance followed by a Dunnett test, a multiple comparison procedure.

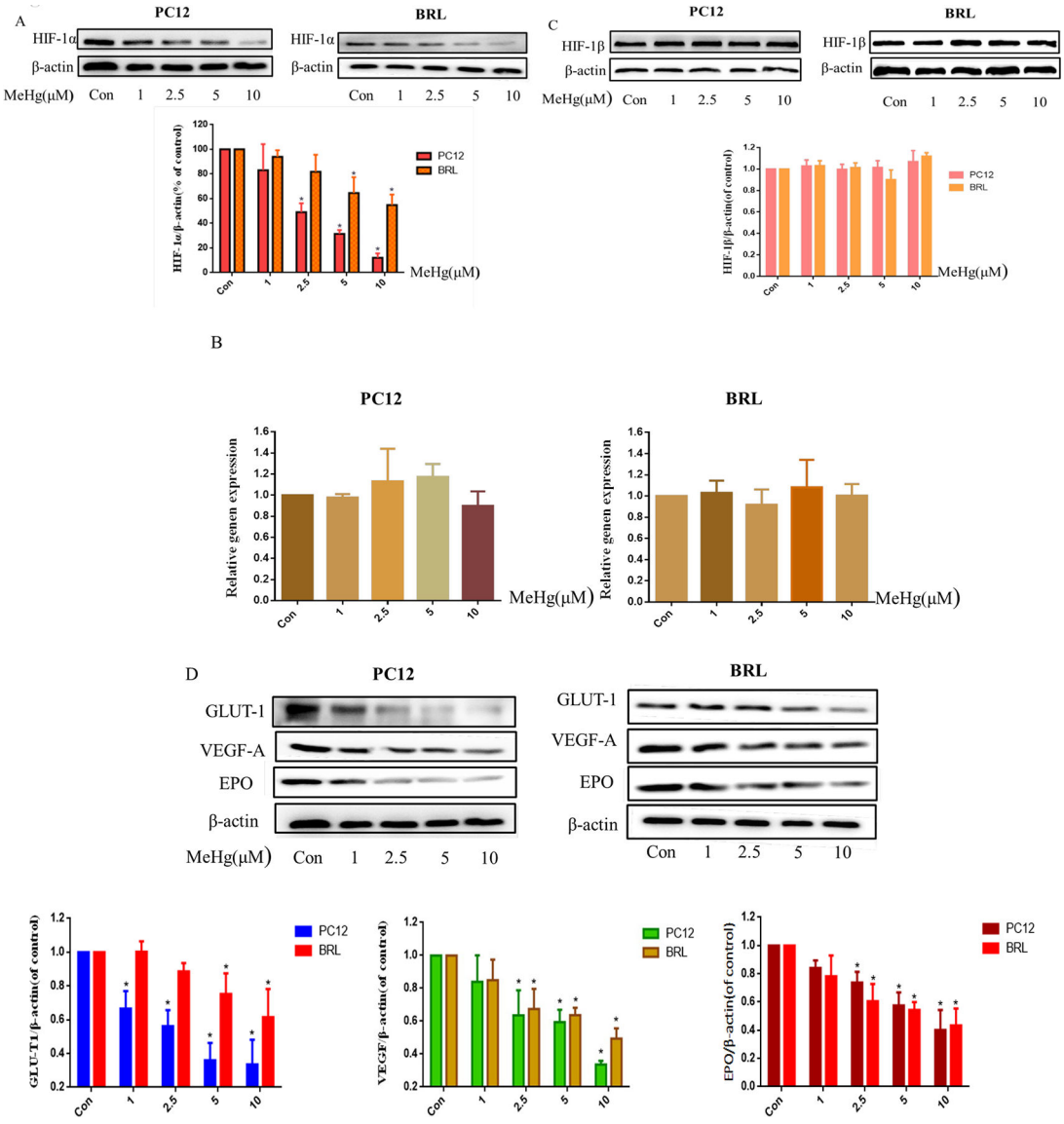


**Fig. 2.**

Protein levels of HIF-1α and its downstream targets in PC12 and BRL cells after treatment with methylmercury (MeHg). A) Western blotting of HIF-1α in cells treated with different concentrations (1–10 μM) of MeHg for 0.5 h. B) Quantitative RT-PCR was used to measure HIF-1α mRNA expression. C) Western blotting was used to detect the protein level of HIF-1β. D) The downstream proteins of HIF-1α glucose transporter-1 (GLUT-1), vascular endothelial growth factor-A (VEGF-A), and erythropoietin (EPO) after exposure to various concentrations (1–10 μM) of MeHg. β-Actin served as a loading control. Data show mean ± standard deviation (n = 3).

*$p < 0.05$, compared with the control group. Control groups were treated with free media without any agents. Statistical analysis was performed by one-way analysis of variance followed by a Dunnett test, a multiple comparison procedure.

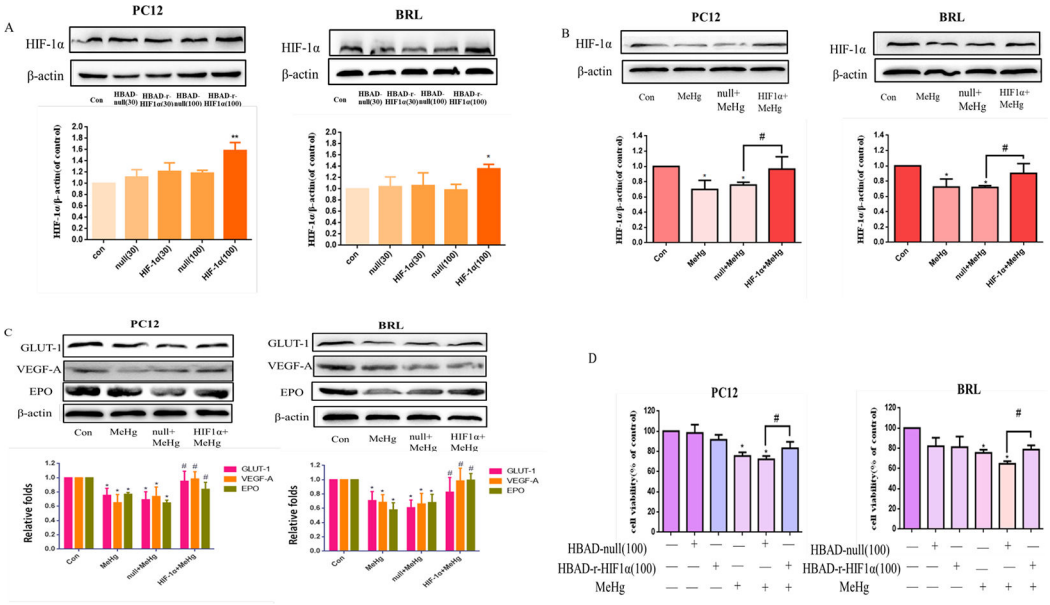


**Fig. 3.**

Effects of adenoviral overexpression of HIF-1α on methylmercury (MeHg)-induced acute cell injury in PC12 and BRL cells. A) Western blotting of HIF-1α protein in cells after 48 hours of transfection with commercially available HIF-1α or control adenovirus. B, C) Transfected cells were treated with MeHg (10 μM for 0.5 hours), followed by western blot analysis of HIF-1β and downstream proteins glucose transporter-1 (GLUT-1), vascular endothelial growth factor-A (VEGF-A), and erythropoietin (EPO). D) Cell viability was measured by MTT assay. $*p < 0.05$, compared with the control group; $^{\#}p < 0.05$, compared with null+MeHg group. Control groups were treated with free media without any agents. Statistical analysis was performed by one-way analysis of variance followed by a Dunnett test, a multiple comparison procedure.

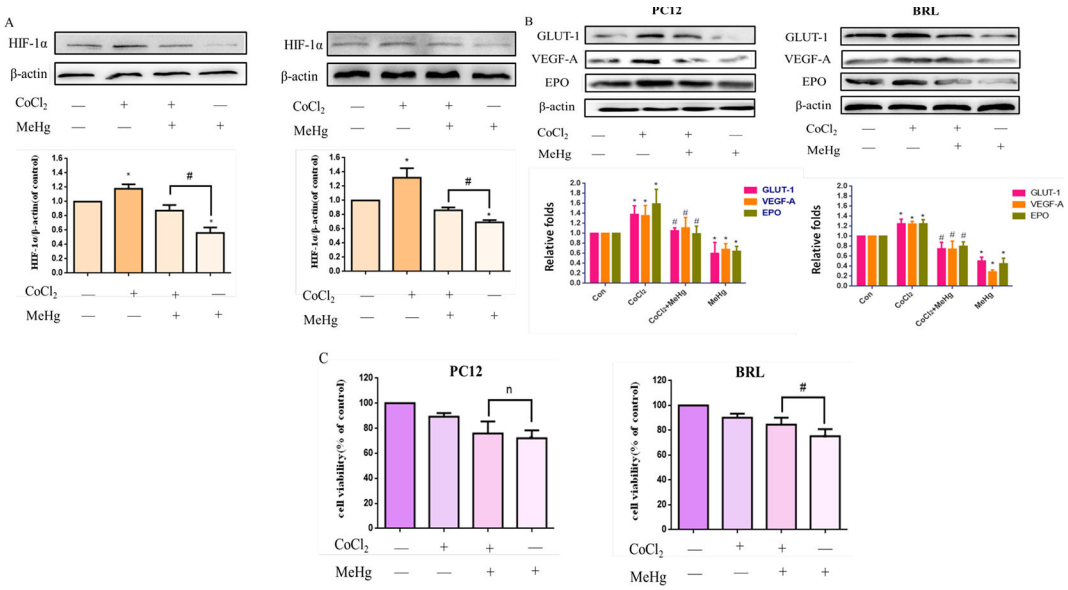


**Fig. 4.**

Effects of cobalt chloride ($CoCl_2$) on methylmercury (MeHg)-induced acute cell injury. PC12 and BRL cells were grown with or without pretreatment with $CoCl_2$ (200 μM for 0.5 h) followed by treatment with MeHg (10 μM). A, B) Protein expression of HIF-1α and downstream targets glucose transporter-1 (GLUT-1), vascular endothelial growth factor-A (VEGF-A), and erythropoietin (EPO) was analyzed by western blotting. β-Actin served as the loading control. C). Cell viability was measured by MTT assay. Data show mean ± standard deviation (n = 3). $^{*}p < 0.05$, compared with the control group; $^{\#}p < 0.05$, compared with the MeHg group. n, no significance compared with the MeHg group. Control groups were treated with free media without any agents. Statistical analysis was performed by one-way analysis of variance followed by a Dunnett test, a multiple comparison procedure.

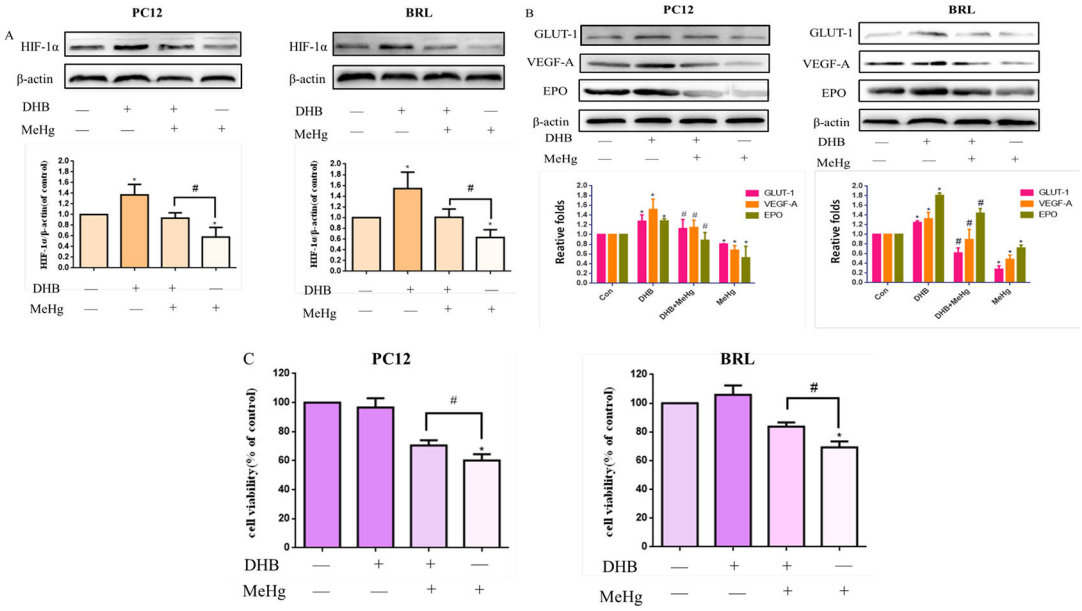


**Fig. 5.**

Effects of 3, 4-Dihydroxybenzoic acid (DHB) on methylmercury (MeHg)-induced acute cell injury. PC12 and BRL cells were pretreated with DHB (1 mM for 6 h), followed by treatment with MeHg. A, B) Protein expression of HIF-1α and downstream targets glucose transporter-1 (GLUT-1), vascular endothelial growth factor-A (VEGF-A), and erythropoietin (EPO) was analyzed by western blotting. β-Actin served as the loading control. C) Cell viability was measured by MTT assay. $^{*}p < 0.05$, compared with the control group; $^{\#}p < 0.05$, compared with the MeHg group. Control groups were treated with free media without any agents. Statistical analysis was performed by one-way analysis of variance followed by a Dunnett test, a multiple comparison procedure.

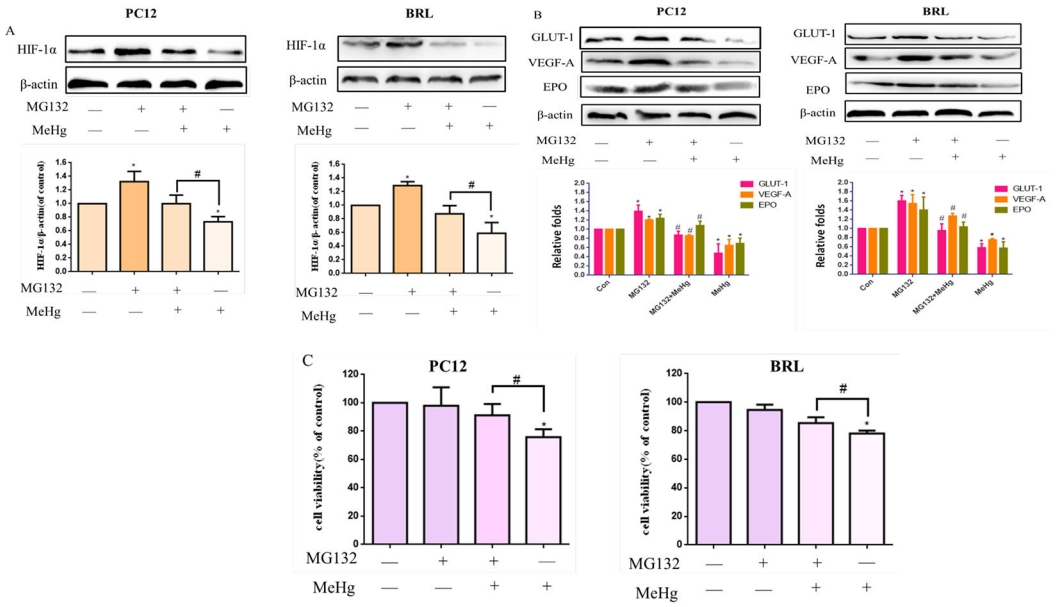


**Fig. 6.**

Effects of MG132 on methylmercury (MeHg)-induced acute cell injury in PC12 and BRL cells. Cells were pretreated with or without MG132 (1 μM for 24 h), followed by treatment with MeHg. A, B) Protein expression of HIF-1α and downstream targets glucose transporter-1 (GLUT-1), vascular endothelial growth factor-A (VEGF-A), and erythropoietin (EPO) was analyzed by western blotting. β-Actin served as the loading control. C) Cell viability was measured by MTT assay. $^{*}p < 0.05$, compared with the control group; $^{\#}p < 0.05$, compared with the MeHg group. Control groups were treated with free media without any agents. Statistical analysis was performed by one-way analysis of variance followed by a Dunnett test, a multiple comparison procedure.

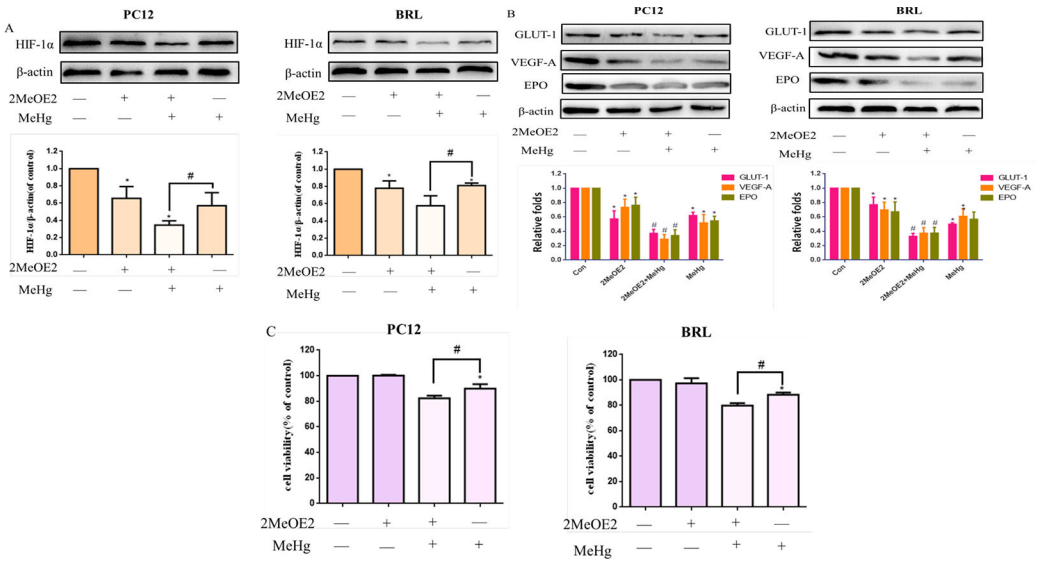


**Fig. 7.**

Effects of 2-methoxyestradiol (2-MeOE2) on methylmercury (MeHg)-induced acute cell injury. PC12 and BRL cells were pretreated with 2-MeOE2 (10 μM for 0.5 hours), followed by treatment with MeHg. A, B) Protein expression of HIF-1α and downstream targets glucose transporter-1 (GLUT-1), vascular endothelial growth factor-A (VEGF-A), and erythropoietin (EPO) was analyzed by western blotting. β-Actin served as the loading control. C) Cell viability was measured by MTT assay. $^{*}p < 0.05$, compared with the control group; $^{\#}p < 0.05$, compared with the MeHg group. Control groups were treated with free media without any agents. Statistical analysis was performed by one-way analysis of variance followed by a Dunnett test, a multiple comparison procedure.